Detection and Location of a Leak in a Gas-Transport Pipeline by a New Acoustic Method

A new method is described for detecting and locating a leak in a gas transport pipeline lying between two pump stations by an indirect acoustic method. The basic concept is to treat the pipeline as an acoustic tube (similar to a wind instrument), and to estimate the impulse response of the acoustic wave in the pipeline solely from the acoustic signal detected at two terminal sites in the pipeline. The test signal introduced at the input site is only acoustic noise; pipeline operation need not be interrupted. If a leak occurs in the pipeline, the impulse response of the acoustic wave in the pipeline has a sharp pulse or a step at a certain time that can be directly related to the site of the leak. Using the mathematical model of the pipeline acoustics, i.e., the wave equation, a theoretical basis is developed to explain how and why the leak can be detected and located. Experiments carried out in the laboratory under conditions comparable to realistic field conditions demonstrate the validity of the proposed detection method.

Kajiro Watanabe
Department of Instrument and Control Engineering
College of Engineering
Hosei University
Koganei, Tokyo, Japan

D. M. Himmelblau
Chemical Engineering Department
University of Texas
Austin, TX 78712

SCOPE

This work pertains to the diagnosis of faults (fault location and identification) in a physically widely dispersed pipeline system. In particular we treat the problem of leak detection and location in a gas-transport pipeline. Existing direct leak detection schemes that aim at locating the points at which leaks occur require human inspection along the pipeline or require that considerable expensive instrumentation be passed through the pipeline; in either case leak detection can be a slow and laborious process. Existing indirect approaches aimed at deciding whether or not a leak exists, and/or localizing the leak site(s), cannot discover the leaking site(s) clearly and accurately.

We have developed a new method that:

1. Requires less effort and uses more economical instrumentation than any of the existing direct methods.
2. Does not require significant interruption of pipeline operation.
3. Can locate leak sites clearly and accurately.

The basic idea underlying the proposed method is derived from the theory of wind instruments. We utilize the fact that the tone of a giant wind instrument (the pipeline) changes in the event of a leak, and we evaluate this change by estimating the acoustic impulse response in the pipeline from acoustic signals detected at the two terminuses of the pipeline.

In addition to explaining the theoretical development that shows why and how the proposed method can detect and locate a leak in a pipeline, we present some experimental results collected under realistic operating conditions that validate the detection theory.

The method proposed here treats the problem of locating one leak at a time in a single pipeline. For the case in which more than one leak occurs at a time, the sites of leaks cannot be uniquely located, but a leak can be located as occurring at one of several possible sites. The number of presumed sites depends on the number of leaks. The theoretical development for the case of multiple leaks is somewhat complicated and is omitted here.

CONCLUSIONS AND SIGNIFICANCE

A new economic method of detecting and locating a leak in an operating gas-transport pipeline is presented. We conclude from the theoretical development of the leak detection method that the impulse responses of an acoustic wave in the pipeline estimated from an acoustic signal measured at two end sites in the pipeline, should show a conspicuous sharp positive or negative pulse or step at a certain time. The leak site can be determined from this pulse or step. Experiments carried out in our laboratory corresponding to realistic pipeline operations have satisfactorily demonstrated that when the theoretical results are applied in practice, leaks can be located. The proposed method has the advantages that it is faster, requires less expensive and heavy instrumentation, and does not require cessation of pipeline operations as do many existing direct leak detection methods; it further has the advantage relative to the existing indirect methods that it can locate leak sites more clearly and precisely.

Introduction

A leak in a gas transport pipeline is always cause for concern, as it may lead to a serious accident and considerable damage may result. In order to prevent such accidents, a way to assure on-line, quick and accurate detection and location of leaks is of major value.

Two general kinds of approaches exist for leak detection, direct approaches and indirect approaches. Direct approaches are those that confirm exact leak sites by inspection together with observation of secondary symptoms such as sound, smell, and visual detection of the abnormal state of vegetation due to the occurrence of leaks. Execution of direct methods is usually carried out by line patrols following pipeline rights-of-way or by local citizens' reports. Thus, most of the research work associated with direct methods has been focused on developing sensitive and accurate detectors for the secondary symptoms. For example, Decker (1978) reported on the effectiveness of a tracer method that detects nitrous oxide outside of a pipeline by surveying it from end to end after nitrous oxide tracer gas is fed into the pipeline inlet. Riemsijk and Bosselarr (1960) and Heim (1979) described a method to locate leak sites by detecting sonic and supersonic sound generated at a leaking site of a high-pressure pipeline. Parker (1980) presented a detailed report describing how the supersonic sound is generated and propagated. Dallavalle et al. (1977) described on-line leak detection (not location) in feedwater preheaters by monitoring the feedwater pressure noise. These direct methods essentially require inspections by human beings to finally confirm the location of the leak site accurately. If the leak sites can be localized to a few areas in the pipeline, the methods are not too costly. Otherwise, they are slow and laborious, and, of course, cannot detect and locate leaks by an on-line, real-time monitoring system.

The indirect approaches to leak detection are based on detecting leaks by measuring inlet-outlet (or spatially sparse) pipeline variables such as pressure and/or volumetric flow rate. The indirect methods originally were based on line balance methods, which investigate the steady state material balance of flow in and flow out and aim at simply detecting the occurrence of leaks, not at locating leak sites. The steady state line balance methods, however, engender some uncertainty. Immediately after changes in the pipeline operating conditions, the transient pressure varies even if no leak occurs, so that such methods can lead to errors in judgment. In order to avoid such error, Goldberg (1979) introduced the dynamic line balance model and reported that the method using his dynamic model demonstrated the ability to detect leaks under a wide range of flow conditions. Huber (1981) introduced a transient line balance model for the same purpose, and Lindsey and Vanelli (1981) also presented a similar model.

Many recent investigations into indirect methods have focused on localizing the leak sites by spatially sparse on-line measurements from the pipeline. Schmidt and Lappus (1980) applied a Luenberger-type observer to the model of a natural gas transport pipeline to find a leak site by estimating all of the state variables in the pipeline from the input and output measurements. Siebert and Isermann (1980) and Siebert (1981) improved and applied the well-known hydraulic gradient method to locate a leak site in a hydraulic pipeline. A typical paper is that by Seiders (1979), who improved on the hydraulic gradient method by subtracting the reference mass flow measured under normal operating condition from the measured mass flow. A cross-correlation method was applied to suppress the effect of noise and to locate a small leak in a pipeline with compressible media such as gas.

Cole (1979) listed patents granted during the period 1935–1976 for leak detection devices that use both direct and indirect techniques. Only one patient refers to the use of multiple microphones to detect sonic waves. Huebler et al. (1982) reported on the use of a single microphone placed inside a low-pressure gas main to detect small leaks. A spectral analysis over the range of 0 to 100 kHz was used to locate the leaks by analyzing the characteristic spectral pattern. Watanabe (1980, 1982) presented a method to locate a leak site by estimating the acoustic propagation in a pipeline using only one microphone set up near the output. These methods are quite interesting, but were mainly theoretical studies to investigate the feasibility of leak detection, and were validated solely by computer simulations or by simplified experiments; the accuracy of location of leak sites was not satisfactory.

The method presented here is a new acoustic method that aims at locating a leak site in a single pipeline by the indirect approach. In the proposed method we estimate the impulse response of the acoustic wave in the leaky pipeline. Information from the impulse response of the acoustic wave in the pipeline locates the leak site.

Theory of the Proposed Acoustic Method

Assumptions

In explaining the principle of the proposed method of acoustic leak detection and location, the following simplifying assumptions are made for the test zone of the pipeline, some of which may not necessarily be fulfilled in actual operation. By the term test zone we mean the part of the pipeline, or the overall pipeline, to which the leak location method is applied.

1. The test zone of the pipeline has two constrictions, one at the input end and one at the output end.
2. The test zone of the pipeline is a single pipe with no branches.
3. Only one leak occurs in the test zone.
4. The test zone of the pipeline has a uniform cross-sectional area for its entire length.
5. The pressure at the input end of the test zone includes random fluctuations whose spectral function is almost white.
6. Pressures inside and near the constrictions in the test zone can be measured by pressure detectors or microphones having limited frequency bands.
7. Acoustic waves propagate in the pipeline without any attenuation and the velocity of gas flow is negligibly small in comparison with the sound velocity.

Assumption 1 is made to provide boundary conditions that let the acoustic wave reflect at the input and output ends of the test zone. Presumably the cross-sectional area of the constrictions is small relative to the cross-sectional area of the pipeline but large enough to permit the gas to flow without excessive pressure drop. In designing a pipeline for commercial service, one should include features for leak detection such as the constrictions themselves, or equivalent equipment that can close to introduce constrictions when a leak-location test is being carried out. Theoretically, another type of boundary condition might possibly be employed instead of constrictions, namely making the input and output of the test zone chamber of wider cross-sectional area than that of the pipeline. For this case, replacing the sound pressure used in the theoretical development outlined below with the fluid element velocity, which can be measured by a gas flow detector, yields the same theoretical results for leak detection. By the term fluid element velocity, we mean alternating gas flow that occurs accompanying sound propagation. If the chambers are at the two ends of the test zone, pipeline operation is not disturbed, but accurate measurements of gas flow are essential.

Assumption 2 is made to avoid the obvious feature that branches can be regarded as leaks.

Assumption 3 is made just to simplify the theoretical development. In practice, the probability that more than two leaks would occur simultaneously in one test zone should be quite low except if the cause of the leaks is something like an earthquake or sudden subsidence.

Assumption 4 is also introduced to make the theoretical development easier. However, a single pipeline usually has only one cross-sectional area for long distances.

Assumption 5 is needed because at the input site of the test zone we need test signal noise with a broad band spectum. If process noise generated by a compressor and/or turbulent flow occurs near the input and has a broad spectrum, that noise can be used as the test signal. Otherwise, suitable noise has to be added at the inlet of the test zone. A variety of methods to generate and add noise at the inlet of the test zone can be employed.

Assumption 6 means that the leak site is to be located solely from changes in the sound pressure in the pipeline measured at the input and output of the test zone. We must take into account the frequency band of the detector as a limiting factor and investigate its effect on leak location.

Assumption 7 means that the gas transport is strictly compressible flow, and the wall of the pipeline is thick, so that essentially no acoustic energy passes through the wall. Because the flow resistance and/or power supplied to transport the gas increases in proportion to the velocity of gas flow, there is always an economically optimal gas flow velocity that is determined by the diameter and length of the pipeline and the properties of the gas. The optimal velocity of gas flow in pipelines in commercial use ($10 \sim 20$ m/s except in pipelines for special purposes) is not high relative to the sound velocity.

Theoretical basis of leak location

Figure 1 shows a sketch of a test zone comprised of a single pipe without branches and with a uniform cross-sectional area as required by assumptions 2 and 4, respectively. A leak may exist as stated in assumption 3. The input and output parts of the test zone contain constrictions as required in assumption 1. The constrictions are realized by placing plates with a centered hole in the pipe. As shown in Figure 1, we let the input end of the test zone be the origin of the x coordinate; the length of the test zone is L. We assume a leak exists at a circular hole at a distance ℓ between the origin and the center of the hole. One side of the circular hole is at a distance ℓ^- and the other is at ℓ^+ so that $\ell^- < \ell < \ell^+$. We assume that the diameter of the leak $(\ell^+ - \ell^-)$ is small relative to ℓ. White noise is added at the input end of the test zone as required in assumption 3, and the acoustic signals excited by the white noise are detected at the input site as $p_i(t)[=p(0,t)]$ and at the output site as $p_o(t)[=p(L,t)]$ by using microphones. We shall show how to locate the leak site ℓ from the measurements $p_i(t)$ and $p_o(t)$.

We divide the pipeline into three parts as follows:

(a) $0 \le x < \ell^-$
(b) $\ell^- \le x < \ell^+$
(c) $\ell^+ \le x \le L$

Because $(\ell^+ - \ell^-) \ll \ell$, we can assume $\ell^+ \simeq \ell^- \simeq \ell$.

To make the theoretical development more general, we first consider the case in which gas flows in the pipeline.

Acoustic characteristics of a pipeline without leaks

Given the first part of assumption 7, namely that the acoustic wave propagates without any attenuation in the pipeline, the wave propagation in the pipeline without leaks can be described by a wave equation of the following form:

$$-\frac{1}{C_f}\frac{\partial f(x,t)}{\partial t} = \frac{\partial f(x,t)}{\partial x}, \quad f(L,t) + b(L,t) = 0 \quad \text{(1a)}$$

$$-\frac{1}{C_b}\frac{\partial b(x,t)}{\partial t} = -\frac{\partial b(x,t)}{\partial x},$$

$$\frac{\rho}{A}[C_f f(0,t) - C_b b(0,t)] = p_i(t) \quad \text{(1b)}$$

where x is the distance from the input site of the test zone; t is the time; $f(x,t)$ and $b(x,t)$ are the fluid element velocity propagating forward and backward, respectively (these veloci-

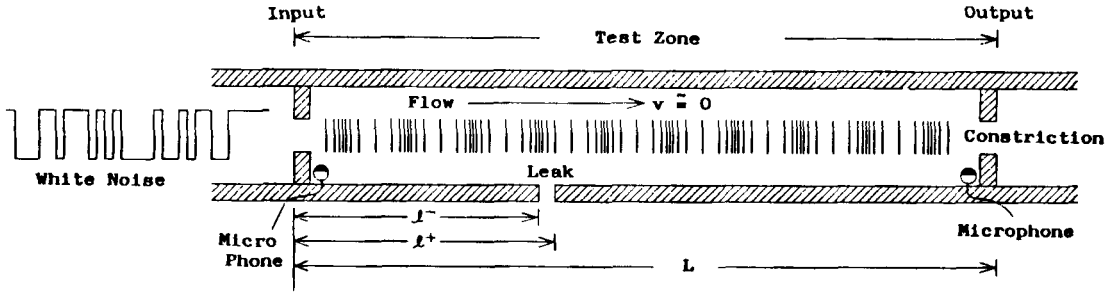

Figure 1. Pipeline test zone.

ties are imaginary and are not measurable); C_f and C_b are the total velocity of sound propagating forward and backward, respectively, and are given by $C_f = C_o + v$ and $C_b = C_o - v$; C_o is the velocity of sound, which is determined by the inside pressure and temperature of the gas; v is the velocity of gas flow; A is the cross-sectional area of the pipe; and ρ is the density of gas.

The total fluid element velocity $u(x, t)$ and the sound pressure $p(x, t)$, which are measurable, are given as follows:

$$u(x, t) = f(x, t) + b(x, t) \tag{1c}$$

$$p(x, t) = \frac{\rho C_f}{A} f(x, t) - \frac{\rho C_b}{A} b(x, t) \tag{1d}$$

When $v = 0$, the two wave equations, Eqs. 1a and 1b, reduce to equations in terms of just two variables, $p(x, t)$ and $u(x, t)$. Fourier transformation of Eqs. 1a–1d with respect to time, and elimination of the terms $f(x, t)$ and $b(x, t)$ from the transformed equations yields the well known four-terminal network relation:

For pipeline section (a) from 0 to ℓ^-:

$$\begin{bmatrix} P(\ell^-, i\omega) \\ U(\ell^-, i\omega) \end{bmatrix} = \boldsymbol{F}(\ell^-) \begin{bmatrix} P(0, i\omega) \\ U(0, i\omega) \end{bmatrix} \tag{2a}$$

For pipeline section (c) from ℓ^+ to L:

$$\begin{bmatrix} P(L, i\omega) \\ U(L, i\omega) \end{bmatrix} = \boldsymbol{F}(L - \ell^+) \begin{bmatrix} P(\ell^+, i\omega) \\ U(\ell^+, i\omega) \end{bmatrix} \tag{2b}$$

where $P(x, i\omega)$ and $U(x, i\omega)$ are the Fourier transforms of $p(x, t)$ and $u(x, t)$, respectively, and the matrix function $\boldsymbol{F}(z)$ is a transfer matrix defined by

$$\boldsymbol{F}(z) = \exp(i\omega z/v') \begin{bmatrix} \cos\left(\frac{\omega z}{C'}\right) - i\left(\frac{v}{C_o}\right)\sin\left(\frac{\omega z}{C'}\right) & -i\frac{\rho C_o}{A}\left(1 - \left(\frac{v}{C_o}\right)^2\right)\sin\left(\frac{\omega z}{C'}\right) \\ -i\frac{\rho A}{C_o}\sin\left(\frac{\omega z}{C'}\right) & \cos\frac{\omega z}{C'} + i\left(\frac{v}{C_o}\right)\sin\left(\frac{\omega z}{C'}\right) \end{bmatrix} \tag{2c}$$

where ω is the angular frequency; $i = \sqrt{-1}$; $v' = v[(C_o/v)^2 - 1]$; $C' = C_o[1 - (v/C_o)^2]$; $z = \ell^-$ or ℓ^+.

Acoustic characteristics of a leak site

The transfer matrix for pipeline section (b) from ℓ^- to ℓ^+, i.e., the leak site, is given by

$$\begin{bmatrix} P(\ell^+, i\omega) \\ U(\ell^+, i\omega) \end{bmatrix} = \begin{bmatrix} 1 & 0 \\ -1/Z_\ell & 1 \end{bmatrix} \begin{bmatrix} P(\ell^-, i\omega) \\ U(\ell^-, i\omega) \end{bmatrix} \tag{2d}$$

where Z_ℓ is the radiational acoustic impedance of the leak, which is given by the following equation when the acoustic wave is not supersonic (Ohizumi, 1968)

$$Z_\ell \simeq i\omega \frac{8}{3\pi\sqrt{\pi d}\tilde{k}} \tag{2e}$$

where d is the cross-sectional area of the leak and $\tilde{k}$ is the compensating coefficient.

Acoustic characteristics of the overall test zone of the pipeline

Elimination of $P(\ell^-, i\omega)$, $U(\ell^-, i\omega)$, $P(\ell^+, i\omega)$, and $U(\ell^+, i\omega)$ from Eqs. 2a, 2b, and 2d yields an effective transfer matrix

$$\begin{bmatrix} P(L, i\omega) \\ U(L, i\omega) \end{bmatrix} = \boldsymbol{F}(L - \ell^+) \begin{bmatrix} 1 & 0 \\ -1/Z_\ell & 1 \end{bmatrix} \boldsymbol{F}(\ell^-) \begin{bmatrix} P(0, i\omega) \\ U(0, i\omega) \end{bmatrix} = \begin{bmatrix} f_{11} & f_{12} \\ f_{21} & f_{22} \end{bmatrix} \begin{bmatrix} P(0, i\omega) \\ U(0, i\omega) \end{bmatrix} \tag{3a}$$

Based on assumption 1, the pipeline being constricted at $x = L$, i.e., because of the boundary conditions in Eq. 1a, we can let

$$U(L, i\omega) \simeq 0 \tag{3b}$$

Thus, from Eqs. 3a and 3b, we have a transfer function from $P(L, i\omega)$ to $P(0, i\omega)$ in the frequency domain as follows:

$$\begin{aligned} \frac{P(0, i\omega)}{P(L, i\omega)} &= f_{22} = G(i\omega) \\ &= \exp(i\omega L/v') \left(\left\{ 1 + \frac{\rho v}{2Z_\ell A}\left[1 - \left(\frac{v}{C_o}\right)^2\right] \right\} \cos\frac{\omega L}{C'} \right. \\ &\quad + i\left\{ \frac{v}{C_o} + \frac{\rho v}{2Z_\ell A}\left[1 - \left(\frac{v}{C_o}\right)^2\right] \right\} \sin\frac{\omega L}{C'} \\ &\quad \left. + i\frac{\rho}{2Z_\ell}\frac{C_o}{A}\left[1 - \left(\frac{v}{C_o}\right)^2\right] \sin\frac{\omega(2\ell - L)}{C'} - \frac{\rho v}{2Z_\ell A} \right. \\ &\quad \left. \times \left[1 - \left(\frac{v}{C_o}\right)^2\right] \cos\frac{\omega(2\ell - L)}{C'} \right) \end{aligned} \tag{4a}$$

If $v \simeq 0$, Eq. 4a can be rewritten as follows:

$$G(i\omega) = \cos\frac{\omega L}{C_o} + \frac{K}{\omega}\sin\frac{\omega L}{C_o} + \frac{K}{\omega}\sin\frac{\omega(2\ell - L)}{C_o}, \quad \text{with} \quad K = \frac{3\pi\sqrt{\pi d\tilde{k}}C_o}{16A} \tag{4b}$$

The transfer function, Eq. 4b, is a real function including a periodic term (the first term) and damped periodic terms (the second and third terms) of frequency ω. The third term in Eq. 4b, which includes the parameter ℓ, has the longest period $\pi C_o/|2\ell - L|$ of damped periodic oscillation among the three terms, and the leak site ℓ is obtained from the value of the longest period and its sign by solving the following equation:

$$\pi C_o/|2\ell - L| = \text{the longest period extracted} \tag{4c}$$

Enhancement of information about the leak site in the transfer function

Extraction of the longest period and its sign from the damped oscillatory response itself involves difficulties, especially when the response is given by the summation of several functions as in Eq. 4b and is corrupted by noise. The frequency response $G(i\omega)$ estimated from the measurements $p_i(t)$ and $p_o(t)$ by calculating $\mathcal{F}[p_i(t)]/\mathcal{F}[p_o(t)]$ also includes such a difficulty. (The symbol $\mathcal{F}[\cdot]$ is the Fourier integral.)

Thus to avoid difficulty in extracting the required data from the estimated $G(i\omega)$, we apply Fourier analysis to the curve $G(i\omega)$ so that the longest period and sign can be obtained more directly. Because Eq. 4b is a real spectral function, we apply the inverse Fourier cosine transform to $G(i\omega)$, which plays the same role as the Fourier cosine transform itself. To make the discussion fit in with assumption 6, we obtain the inverse Fourier transform for the limited frequency band width $\omega_l \le \omega \le \omega_h$. The inverse Fourier cosine transform becomes

$$\begin{aligned} g(t) &= \frac{2}{\pi}\int_{\omega_l}^{\omega_h} G(i\omega)\cos\omega t d\omega \\ &= \frac{2}{\pi}\int_{\omega_l}^{\omega_h}\cos\frac{\omega L}{C_o}\cos\omega t d\omega \\ &\quad + \frac{2K}{\pi}\int_{\omega_l}^{\omega_h}\frac{\sin\dfrac{\omega L}{C_o}}{\omega}\cos\omega t\, d\omega \\ &\quad + \frac{2K}{\pi}\int_{\omega_l}^{\omega_h}\frac{\sin\dfrac{\omega(2\ell - L)}{C_o}}{\omega}\cos\omega t\, d\omega \\ &= g_1(t) + g_2(t) + g_3(t) \end{aligned} \tag{4d}$$

where $g_1(t)$, $g_2(t)$, and $g_3(t)$ correspond to the first, second, and third inverse Fourier cosine transforms listed in Eq. 4d, respectively. The first term, $g_1(t)$, shows a sharp positive pulse, and the second term, $g_2(t)$, shows a positive pulse (when ω_l is large and frequency band width $\omega_h - \omega_l$ is narrow) or a negative step (when $\omega_l \to 0$ and $\omega_h \to \infty$) at time $t_L = L/C_o$. The third term, $g_3(t)$, shows a sharp positive or negative pulse or step at time $t_\ell = |2\ell - L|/C_o$. The pulse $g_1(t)$ becomes sharper and the shapes of $g_2(t)$ and $g_3(t)$ change from pulse form to step form as $\omega_h - \omega_l$ is increased and as $\omega_l \to 0$.

If $\ell_1 < L/2$, the third term in Eq. 4b from which the leak site is determined, can be rewritten as

$$\frac{K}{\omega}\sin\frac{\omega(2\ell_1 - L)}{C_o} = -\frac{K}{\omega}\sin\frac{\omega(L - 2\ell_1)}{C_o} \tag{4e}$$

Thus, the inverse Fourier cosine transform has a negative sharp pulse or a positive step at time

$$t_{\ell 1} = \frac{L - 2\ell_1}{C_o} \tag{4f}$$

which leads to Eq. 5a. By using the relation $t_L = L/C_o$ estimated from experiment, ℓ_1 can be calculated from the second statement in Eq. 5a:

$$\ell_1 = \frac{1}{2}(L - C_o t_{\ell 1}) = \frac{L}{2}\left(1 - \frac{t_{\ell 1}}{t_L}\right) \tag{5a}$$

Similarly, if $g(t)$ has a positive sharp pulse or a negative step at $t = t_{\ell 2}$, the leak site must be at $\ell_2 \ge L/2$ and the site can be determined from

$$\ell_2 = \frac{1}{2}(L + C_o t_{\ell 2}) = \frac{L}{2}\left(1 + \frac{t_{\ell 2}}{t_L}\right) \tag{5b}$$

Figure 2 demonstrates the relation between the leak site and the time when the pulse or the step occurs in $g(t)$.

Procedure to Locate a Leak

Conditions for measurements

Here we describe how to execute a leak location strategy based on the theoretical results obtained in the previous section. The theory was developed for the time-continuous data $p_i(t)$

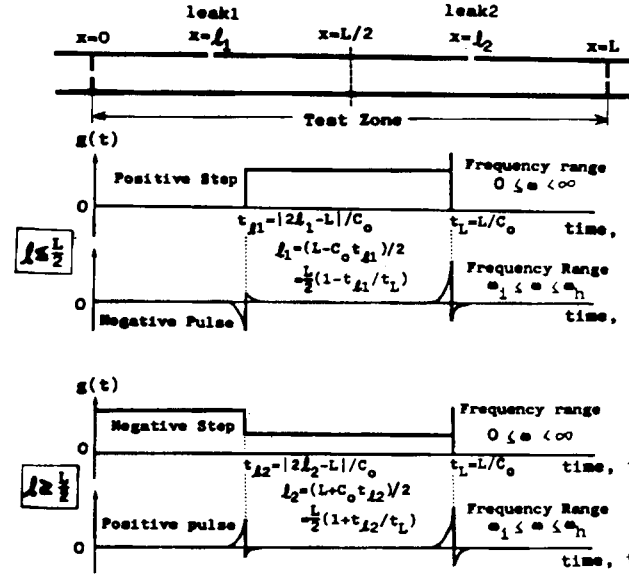

Figure 2. Relation between leak sites and impulse response.

and $p_o(t)$. In practice, however, data will be measured discretely, because digital computation for the leak location can be carried out easier than analog computation.

We first consider how to select the sampling interval τ and/or the maximum frequency ω_m of the noise generated at the input end, and determine the characteristics of the acoustic detectors set up at each of the two ends of the pipeline.

Let Δx be length of a unit pipe; Δx is the shortest permissible length of pipe that enables one to identify the leak site. Let M be the number of unit pipes that compose the entire test zone of the pipeline. The parameters τ, Δx, ω_m, and M are related to each other.

From Eqs. 5a, b, which relate the leak site and the time of occurrence of the pulse or step, by halving the sampling interval τ, with the pipeline discretized with respect to length, the unit length is given by

$$\Delta x = \frac{\tau C_o}{2} \quad \text{which yields} \quad \tau = \frac{2\Delta x}{C_o} \tag{6a}$$

Suppose τ is selected to satisfy Shannon's sampling theorem; then the relation between ω_m and τ is

$$\omega_m = \pi/\tau \quad \text{or} \quad \tau = \pi/\omega_m \tag{6b}$$

Further, L, M, and Δx are obviously related as follows:

$$M = L/\Delta x \quad \text{or} \quad \Delta x = L/M \tag{6c}$$

Thus, if one of the parameters (τ, Δx, ω_m, M) is known, the remaining parameters are determined uniquely. Then, instead of considering how to select τ, we consider instead how to select ω_m. From Eqs. 6a and 6b, the relation between Δx and ω_m is

$$\Delta x = (\pi C_o/2\omega_m) \tag{6d}$$

Equation 6d indicates that the choice of a larger value of ω_m yields a higher resolution of identifiability of the leak site, which is, of course, desirable. However, the third term of Eq. 4b including the leak site ℓ shows a damped oscillatory response. Thus, with a value of ω greater than a certain value, the third term becomes negligibly small in comparison with the level of noise. Let

$$\text{Magnitude of the term } \frac{K}{\omega}\sin\frac{\omega(2\ell - L)}{C_o} = \frac{K}{\omega}\sin\frac{\omega(2\ell - L)}{C_o}\bigg|_{\omega=0} = K\frac{(2\ell - L)}{C_o} = \left[K\frac{(2\ell/L) - 1}{C_o}\right]L = \frac{3\pi\sqrt{\pi}(2\ell - L)\tilde{k}}{16A}\sqrt{d} \tag{6e}$$

Then the frequency range in which magnitude of the spectrum of the third term in Eq. 4b is greater than 5% of the magnitude $K(2\ell - L)/C_o$, i.e.,

$$0.05\left|K\frac{2\ell - L}{C_o}\right| \le \left|\frac{K}{\omega}\sin\frac{\omega(2\ell - L)}{C_o}\right| \tag{6f}$$

is obtained as

$$0 \le \omega \le \frac{5.67\pi C_o}{|2\ell - L|} = \frac{5.67\pi C_o}{|(2\ell/L) - 1|}\frac{1}{L} \tag{6g}$$

From Eq. 6e and Eq. 6g, we can observe:

1. As $\ell \to (L/2)$, the magnitude of $[K(2\ell - L)/C_o] \to 0$ and the upper bound of the frequency range $[5.67\pi C_o/(2\ell - L)] \to \infty$. Thus, if $\ell \to (L/2)$, identification of the leak site becomes difficult. Conversely, identification of a leak that occurs where $\ell \to 0$ or $\ell \to L$ is easy. In the case $\ell \simeq L/2$, the difficulty in locating a leak can be overcome by a test strategy involving more than one location for the downstream microphone.

2. For a fixed $\ell/L(\neq 0.5)$, as the length L of the test zone increases, the magnitude $[K(\ell/L - 1)/C_o]L$ increases, and the upper bound $[(5.67\pi C_o)/(|2\ell/L - 1|/L)]$ of the frequency range decreases. Thus if L is long, the third term of Eq. 4b must be identified by test noise with a low range of frequency.

3. From the last statement in Eq. 6e, for a leak with a constant cross-sectional area the magnitude decreases in proportion to the cross-sectional area A of the pipeline. This means that location of a small leak in a pipeline with a large cross-sectional area is more difficult than in a pipeline with a smaller cross-sectional area.

Let us look at some specific calculations for the magnitude. Let $\ell/L = 0.45$ or $\ell/L = 0.55$. Then the magnitude given by Eq. 6e and the upper bound of the frequency range given by Eq. 6g become, respectively,

$$K\left(\frac{2\ell - L}{C_o}\right) = \frac{K}{10C_o}L, \quad \frac{5.67\pi C_o}{|(2\ell/L) - 1|L} = \frac{56.7\pi C_o}{L} \tag{6h}$$

Then in this case, the frequency range should be

$$0 \le \omega \le \omega_m, \quad \omega_m \ge \frac{56.7\pi C_o}{L} \tag{6i}$$

Equation 6i can serve as a guideline for selecting the noise generator and the acoustic detectors. To be specific, their frequency response should be flat for the frequency range given by Eq. 6i. Note that choosing a much larger value of ω_m than $56.7\pi C_o/L$ yields inaccurate estimation of the transfer function, Eq. 4b, because local sources of noise caught by one of the acoustic detectors will be of too high a frequency to propagate satisfactorily to the other detector. Local sources of noise might be:

- The high-frequency part of an external noise source in the pipeline
- Pump noise
- Compressor noise
- Noise that might come from pipe vibration due to the leak itself (in the 500~800 Hz range)
- Noise due to the impact of gas on the soil surrounding the pipe (20~250 Hz).

Suppose we select $\omega_m = 56.7\pi C_o/L$; then we obtain

$$\tau = L/56.7C_o, \quad \Delta x = L/113.4, \quad M = 56.7 \tag{6j}$$

The number of data N collected should be determined in the following way. If $\ell/L = 0$ or $\ell/L = 1$, the period of the third term of Eq. 4b becomes $2\pi C_o/L$. The minimum width $\Delta\omega$ of fre-

quency should be much less than the period, i.e.,

$$2\pi \frac{C_o}{L} \gg \Delta\omega = \frac{2\pi}{N\tau} \tag{6k}$$

which leads to

$$N \gg \frac{1}{\tau C_o} = \frac{\omega_m L}{\pi C_o} \tag{6l}$$

From Eq. 6k, as N increases $\Delta\omega$ becomes smaller, enabling the more accurate location of a leak site.

Use of process noise or a sinusoidal signal as the test signal

Inherent process noise such as compressor noise, turbulent noise, and valve noise can be used as the test signal if the noise is generated near the input end of the test zone and if the spectrum of the noise has sufficiently high power and is flat in the frequency range given by Eq. 6i.

A sinusoidal signal can be used instead of noise to estimate the transfer function, Eq. 4b. Use of a sinusoidal signal yields a better estimate in a noisy pipeline. However, estimation of the transfer function by using a sinusoidal signal is quite time-consuming and tedious. Furthermore, a sine wave generator with a resolution of $\Delta\omega$ (if L is long) is an expensive piece of equipment.

Calculation of the frequency and impulse responses

The frequency response $G(m)[=G(i2\pi m/N\tau)]$ corresponding to Eq. 4b and the impulse response $g(k)[=g(k\tau)]$ corresponding to Eq. 4d can be obtained by applying Fourier analysis to the discrete data $p_i(t)$ and $p_o(t)$ (measured using the criteria described above). Because $p_i(t)$ and $p_o(t)$ are measured discretely, we employ the discrete Fourier transform (DFT) and the inverse discrete Fourier transform (IDFT). Both can be executed very quickly by the fast Fourier transform (FFT) algorithm.

Define k as the discrete time with the sampling interval τ; m is the discrete frequency with step $\Delta\omega = (2\pi/N\tau)$; $p_i(k)$ and $p_o(k)$ are the discrete measurements of the input and output data, respectively. Then the calculation procedure to get the impulse response $g(k)$ using the DFT and IDFT operations is as follows.

1. First calculate:

$$\tilde{G}(m) = \frac{\text{DFT}[p_i(k)]}{\text{DFT}(p_o(k))} \tag{7a}$$

2. Then obtain:

$$\begin{aligned}\overline{G}(m) = \frac{1}{429}\{&-36[\tilde{G}(m-5)+\tilde{G}(m+5)]\\ &+9[\tilde{G}(m-4)+\tilde{G}(m+4)]\\ &+44[\tilde{G}(m-3)+\tilde{G}(m+3)]\\ &+69[\tilde{G}(m-2)+\tilde{G}(m+2)]\\ &+84[\tilde{G}(m-1)+\tilde{G}(m+1)]\\ &+89\tilde{G}(m)\} \equiv W[\tilde{G}(m)]\end{aligned} \tag{7b}$$

where $W(\cdot)$ stands for a window, and select $\hat{G}(m)$ as

$$\hat{G}(m) = \begin{cases}\overline{G}(m) & \text{if } |\tilde{G}(m)|>2|\overline{G}(m)| \\ \text{otherwise} & \tilde{G}(m)\end{cases} \tag{7c}$$

The logic of Eq. 7c avoids ill effects due to division by DFT $[p_o(k)]$ in Eq. 7a. Note that from Eq. 4b, $G(i\omega)$ is given by the summation of $\cos(\omega L/C_o)$, $(K/\omega)\sin(\omega L/C_o)$, and $(K/\omega)\sin[\omega(2\ell - L)/C_o]$ so that $G(i\omega)$ must be bounded above and below by a certain value. However, $\tilde{G}(m)$ in Eq. 7a can have big values in the form of a pulse at some m due to division by zero in the calculation of Eq. 7a. The operation in Eq. 7c is designed to suppress such big pulses.

3. Apply a window operation:

From Eq. 4b, we know that $G(i\omega)$ is a continuous smooth function. Thus, a window that substantially suppresses small fluctuations in $\hat{G}(m)$ can be applied effectively. We applied a window $W(\cdot)$, which is the same operation as Eq. 7b and is a spectrum window that makes $\hat{G}(m)$ smooth (in the sense of a least-squares error) for the period $[(m-5),(m+5)]$,

$$G(m) = W[\hat{G}(m)] \tag{7d}$$

4. Calculate $g(k)$:

Recall from Eq. 4b that $G(i\omega)$ is real. Thus, the impulse response $g(k)$ can be obtained by applying the inverse Fourier cosine transform. Let $Re[G(m)]$ be the real part of a complex number $G(m)$. Then the inverse Fourier cosine transform for the discrete data can be calculated by using the IDFT as follows:

$$g(k) = \text{IDFT}\{Re[G(m)] + i0\} \tag{7e}$$

Experimental

Experimental system

Experiments were carried out using the laboratory pipeline shown in Figure 3a. The pipeline was constructed by using 19 sections of iron pipe about 2.75 m long and 18 PVC junctions each about 0.4 m long. The inside diameter of the pipe was 22.1 mm (the cross-sectional area A was 3.83×10^{-4} m^2). The length L of the test zone was selected to be 58.8 m. The input and output of the test zone were constricted by two plates each with a 10 mm dia. centered hole. Experiments were carried out when the temperature was 291 K (19°C), i.e., the sound velocity was C_o = 344 m/s, for three cases:

1. A circular leak was cut at ℓ = 2.18 m
2. Leak 1 was closed and a circular leak was cut at ℓ = 17.73 m
3. Leaks 1 and 2 were closed and a circular leak was cut at ℓ = 39.76 m.

All the leaks had the same cross-sectional area, the diameter of the hole being $d = 1.96 \times 10^{-5}$ m^2. Gas did not flow in the pipe during the test.

Noise generated by a 17-bit, M-sequence noise generator with a clock time of 1 ms, amplified by an AC amplifier and actuated by a loudspeaker with the frequency response shown in Figure 3b, was added at the input site of the test zone of the pipeline. The frequency responses of microphones *1* and *2* were

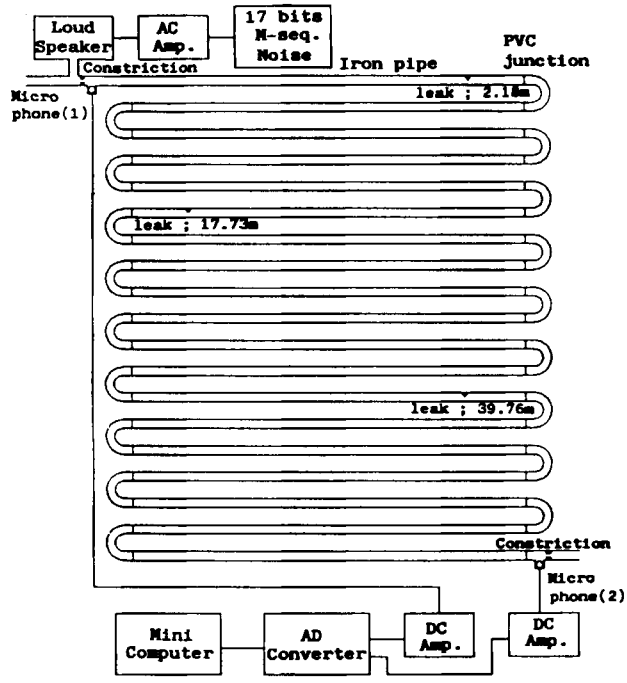

Figure 3a. Experimental system.

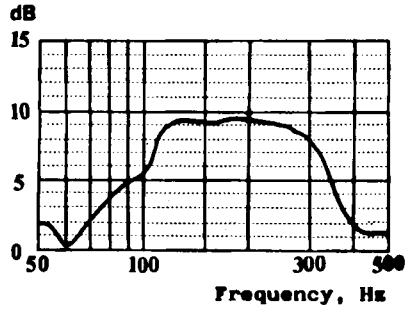

Figure 3b. Frequency response of loudspeaker used as a noise source.

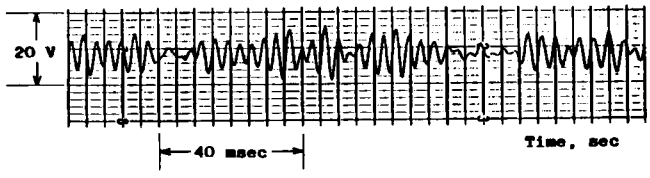

Figure 3c. Measurement of $p_i(t)$ by microphone 1 for a leak at $\ell = 2.18$ m.

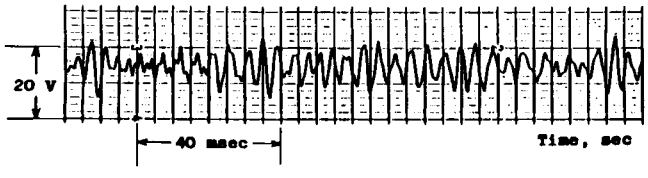

Figure 3d. Measurement $p_o(t)$ by microphone 2 for a leak at $\ell = 2.18$ m.

flat for the frequency range of the loudspeaker. Thus, from Figure 3b, the frequency band corresponding to $\omega_i \le \omega \le \omega_h$ for integration of Eq. 4d was $\omega_i = 690$ rad/s (110 Hz) $\le \omega \le \omega_h = 2{,}137$ rad/s (340 Hz).

The input signal $p_i(t)$ detected by microphone *1* and the output signal $p_o(t)$ detected by microphone *2* are shown in Figures 3c and 3d, respectively, for a leak at $\ell = 2.18$ m.

The signals $p_i(t)$ and $p_o(t)$ were discretized with a sampling interval of $\tau = 1.470$ ms by a 12-bit analog-digital (AD) converter for which the holdover frequency was 2,137 rad/s, a value that is almost equal to ω_h of the loudspeaker. The number N of discrete data points equaled 2,048.

Suppose that $\omega_h = \omega_m = 2{,}137$ rad/s. That the above choice of τ and N satisfies the conditions of Eqs. 6i, 6b, and 6l can be seen as follows:

$$\omega_m = 2{,}137 \text{ rad/s} \gg (56.7\pi C_o/L) = 1{,}042 \text{ rad/s}$$

$$\tau = (\pi/\omega_m) = 1.470 \text{ ms}$$

$$N = 2{,}048 \gg (\omega_m L/\pi C_o) = 116.3$$

Furthermore, the minimum resolution of identifiability of the leak site, Δx, and the number of the unit pipes, M, were:

$$\Delta x = (\tau C_o/2) = 0.253 \text{ m}$$

$$M = L/\Delta x = 232$$

The DC amplifiers used to amplify the signals $p_i(t)$ and $p_o(t)$ were adjusted so that the AD converter worked with full bits.

Simulation results

Before describing the experimental results, we will first describe some results of computer simulations and then compare them with the experimental results. The impulse response function $g(t)$ in Eq. 4d was calculated for the same conditions as used in the experimental system—i.e., $L = 58.8$ m; $C_o = 344$ m/s; $A = 3.83 \times 10^{-4}$ m^2; $d = 1.96 \times 10^{-5}$ m^2; $\omega_i = 960$ rad/s; $\omega_h = 2{,}130$ rad/s; $\tilde{k} = 1$; for each of the three leak sites $\ell = 2.18$ m, $\ell = 17.73$ m, and $\ell = 39.76$ m, respectively.

Based on the theory for leak detection and location, for the case in which the frequency range of measurement is limited and no leak exists, $g(t)$ must have one positive pulse at $t = 0.171$ s corresponding to L/C_o. For the cases in which a leak exists, $g(t)$ must have two pulses. One pulse must be positive and must appear at $t = 0.171$ s, corresponding to L/C_o; the other must be either positive or negative corresponding to a particular leak site as follows:

- For $\ell = 2.18$ m, $g(t)$ must have a negative pulse at $t_\ell = 0.158$ s
- For $\ell = 17.73$ m, $g(t)$ must have a negative pulse at $t_\ell = 0.0678$ s
- For $\ell = 39.76$ m, $g(t)$ must have a positive pulse at $t_\ell = 0.602$ s.

The simulation results indicated by the open circles in Figures 4a–d demonstrate that the correct positive or negative pulses occurred at the correct times for each leak site.

From observation 1 in the earlier section Conditions for Measurements, the magnitude of the pulse $\to 0$ as $\ell \to L/2$, and the

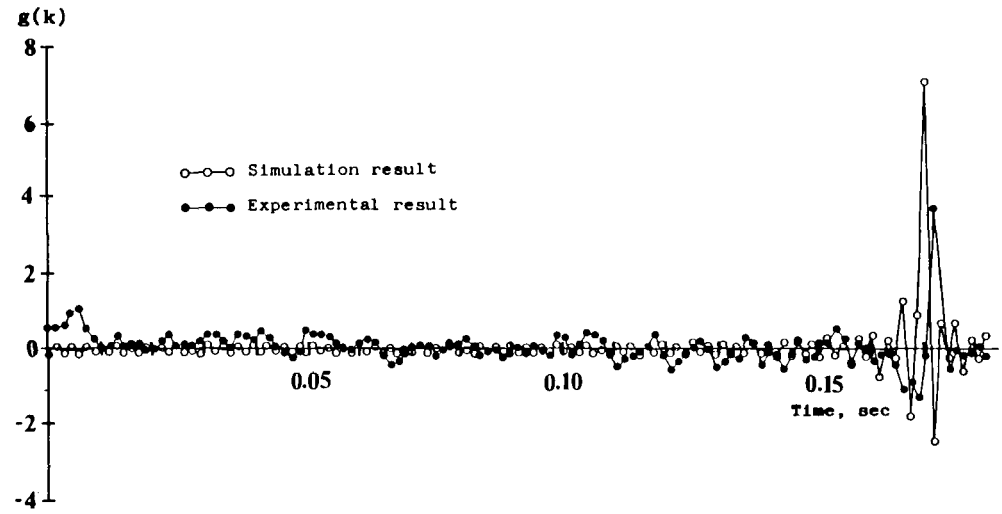

Figure 4a. Simulation and experimental results for impulse response $g(k)$ when no leak existed.
According to theory, only one pulse at $t = 0.171$ s should occur.

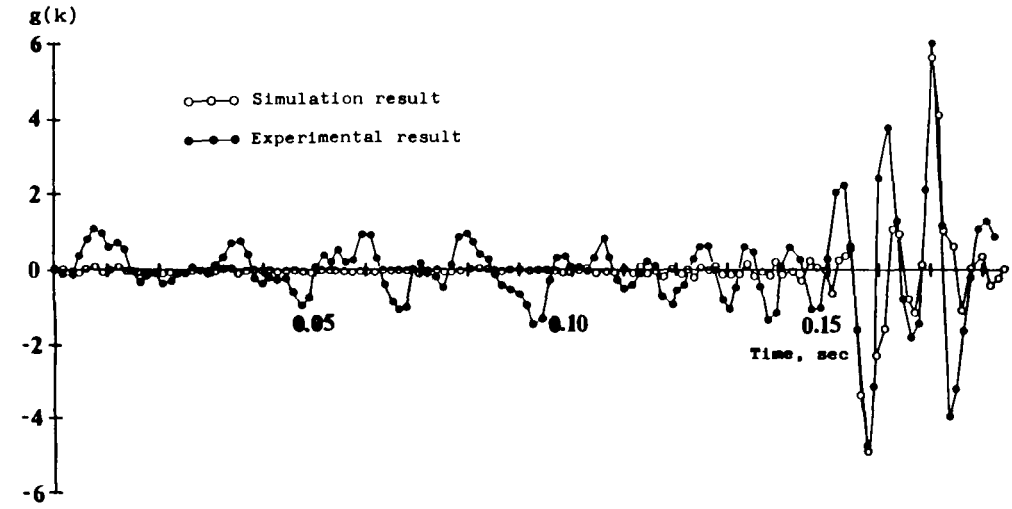

Figure 4b. Simulation and experimental results for impulse response with a leak at $\ell = 2.18$ m.
t_ℓ should be 0.158 s.

magnitude becomes greater as $\ell \to 0$ or L. The simulation results demonstrated the same tendency. The value of the magnitude itself is a relative value and has no particular meaning.

Experimental results

Experiments were carried out using the system shown in Figure 3a, and the data obtained by the experiments were processed by the procedure outlined in connection with Eqs. 7a–7e. From the leak detection theory and the simulations described in the previous section, pulses such as shown in Figure 2 and denoted by the open circles in Figures 4a–d should occur. The function $g(t)$ or $g(k)$ should have at most two pulses in the period $0 \le t \le L/C_o$, and one of them must occur at $t = t_L = L/C_o$. Furthermore, from the simulation results, the pulses should be larger and sharper than the amplitudes of the oscillations occurring in the vicinity of the times at which the pulses are observed. Thus, we selected the two biggest pulses for the estimated impulse response $g(k)$ for the interval $0 \le t \le L/C_o = 0.171$ s. Responses given by the filled circles in Figures 4a–d show the impulse response $g(k)$ obtained experimentally for the three different leaks described above.

The response shown by filled circles in Figure 4a is for the case in which no leak existed. As expected, the estimated impulse response $g(k)$ had a sharp pulse at $t_L \simeq 0.171$ s. No other big pulses were noted for the period $0 \le t \le t_L = 0.171$ s.

Responses shown by filled circles in Figures 4b–d represent the impulse responses for cases in which the pipeline had a leak. Every impulse response exhibited several pulses. For the interval $0 \le t \le 0.171$ s, the sharpest and biggest pulse was at or around $t = 0.171$ s, corresponding to L/C_o. The second biggest pulse was that which corresponded to $t = |2\ell - L|/C_o$. The response in Figure 4b shows that $g(k)$ had the second biggest pulse, one with a negative amplitude, at $t = 0.157$ s. Because the second biggest pulse was negative, from Eq. 5a the leak site ℓ was estimated to be 2.39 m (vs. the actual distance of $\ell = 2.18$ m). The response in Figure 4c shows that $g(k)$ had the second biggest pulse, one with a negative amplitude, at $t = 0.0662$ s. Because

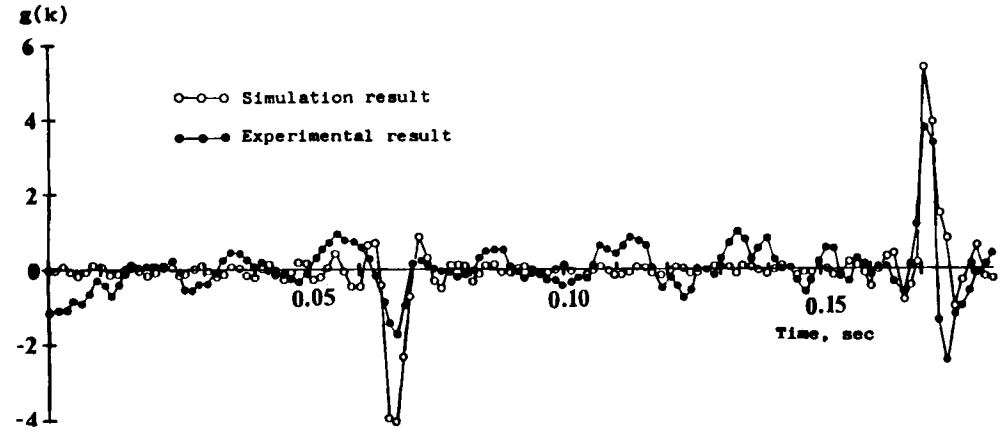

Figure 4c. Simulation and experimental results for impulse response with a leak at ℓ = 17.73 m.
t_ℓ should be 0.0628 s.

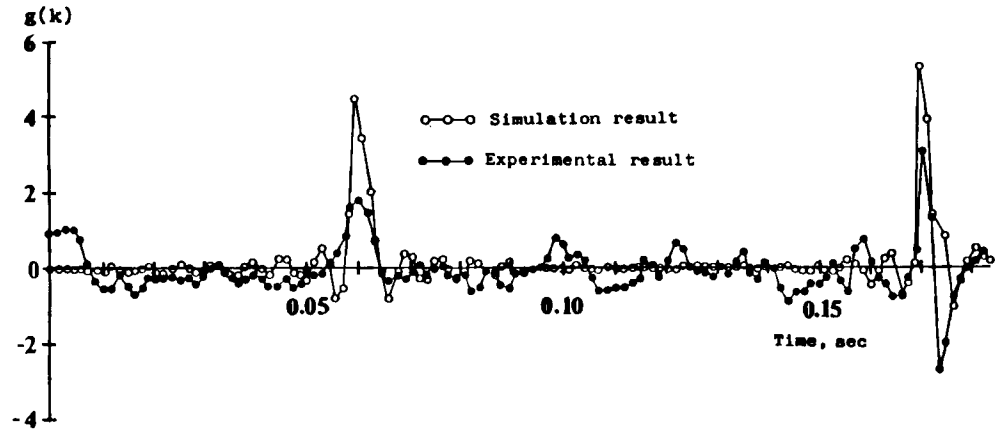

Figure 4d. Simulation and experimental results for impulse response with a leak at ℓ = 39.76 m.
t_ℓ should be 0.0602 s.

the second biggest pulse was negative, from Eq. 5a, the leak site ℓ was estimated to be 18.0 m (vs. ℓ = 17.73 m). Finally, the response in Figure 4d shows that $g(t)$ had the second biggest pulse, one with a positive amplitude, at t = 0.0603 s. Because the second biggest pulse was positive, from Eq. 5b, the leak site ℓ was estimated to be 39.8 m (vs. ℓ = 39.76 m).

The experimental results are quite similar to the simulation results in locating the leak sites. This outcome means that the basic equations used to develop the leak location theory, Eqs. 1a–d and Eq. 2a, were appropriate for the problem, and that the theory is valid. The only difference between the simulation results and the experimental results was that the experiments took place in the presence of noise. In the experiments, the frequency response $G(m)$ was obtained as a stochastic function by using the 17-bit M-sequence noise as a test signal, whereas $G(i\omega)$ corresponding to $G(m)$ calculated from Eq. 4b for the simulations, was deterministic. Thus, if the noise level ever becomes higher than or as significant as the levels of the impulse response, it may be impossible to distinguish the second biggest impulse from the others. To reduce the effect of such extraneous noise, we carried out several replicate experiments. From the estimated impulse responses $g(k)$ for the interval $0 \le t \le L/C$ = 0.171 s, we picked out the two times at which the first and the second clear-out highest pulses occurred (one must occur at L/C_o and the other must occur at $|2\ell - L|/C_o$). The results for all of the experiments were averaged and their frequencies of occurrence normalized. Figures 5a–d illustrate the normalized frequency of occurrence. The resulting frequency plots indicate that it would be easy to discriminate and obtain both the pulse at the end of the pipeline and the occurrence of a leak, if one existed.

Figure 5a demonstrates that the occurrence of the pulses is concentrated at one time, namely t = 0.171 s, that corresponds to L/C_o. The frequency of the other pulses is almost uniformly distributed and substantially lower. Figure 5b shows that the pulses are concentrated at only two times, t = 0.171 s (corresponding to L/C_o) and t_ℓ = 0.157 s (corresponding to $|(2\ell - L)/C_o|$, ℓ = 2.18 m). Figure 5c shows that the pulses are concentrated at only two times, t = 0.171 s and $t \simeq$ 0.0662 (corresponding to $|(2\ell - L)/C_o|$, ℓ = 17.73 m). Figure 5d shows that the pulses are concentrated at t = 0.171 s and t_ℓ = 0.0603 s (corresponding to $|(2\ell - L)/C_o|$, ℓ = 39.76 m).

Thus, even though a single test in some instances may fail to identify a leak site, repeated testing should clearly identify the leak site via frequency counts. Furthermore, the testing can be carried out in real time.

In the experimental setup we used, leaks with a cross-sectional area of less than 7.07×10^{-6} m^2 *could not be located.*

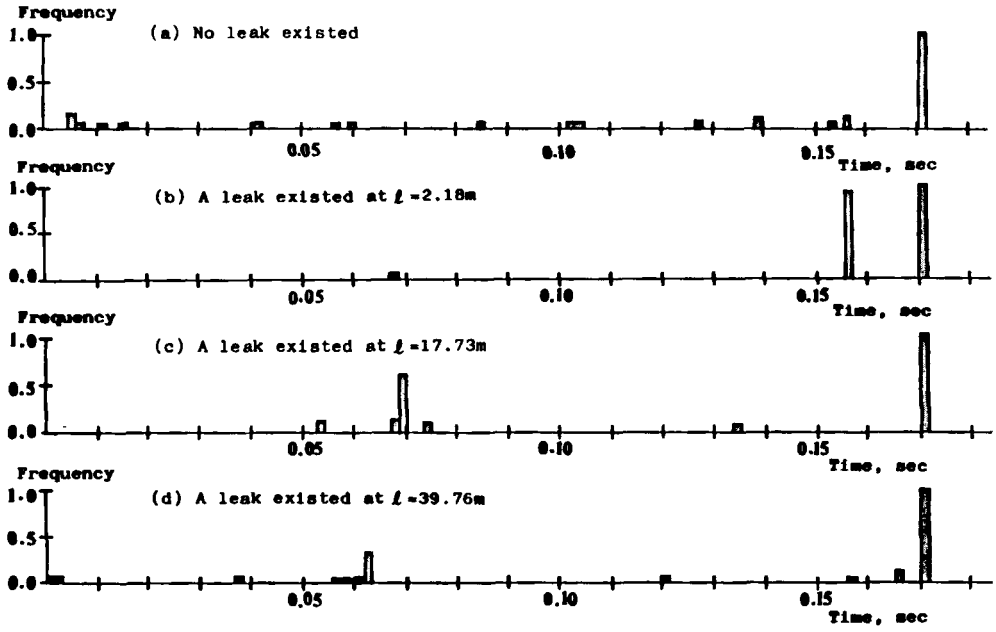

Figure 5. Frequency of times when pulses occur.

Discussion

Minumum detectable size of leaks

Simulation results for the proposed method for the deterministic cases showed that any size leak can be located. In practice, the minimum detectable size of leaks that can be determined is established by the conditions of measurements, i.e.:

- S/N ratio in the measurements
- Frequency range of measurements
- Size of hole of the constrictions.

Of these three conditions, the frequency range of the measurements substantially influences the ability to locate a leak. The third term in Eq. 4b, from which the leak site is identified, is a damped oscillatory function of ω. Thus, accurate measurements in the lower frequency range, for example, 0 Hz ~ 0.5 ω_m (ω_m is defined in Eq. 6i) are more important than measurements in the range 0.5 ω_m ~ ω_m insofar as improving the ability to locate a leak. In experiments, the spectrum of the test signal was limited to 110–340 Hz. A very important part of the frequency, 0–110 Hz, was not available in the experiments because of the type of instruments employed. Thus, by having a noise generator that generates test signals with wider frequency in the lower frequency range, the minimum detectable leak size could have been smaller than that in experiments.

Length of the test zone of the pipeline

The experiments were carried out using a pipeline with a length of 58.8 m and a diameter of 22.1 mm. What happens if the pipeline or the test zone is substantially longer and the cross-sectional area is somewhat wider?

Consider a test zone of 20 km length and 50 cm dia. to locate a leak of diameter of d_ℓ. We assume that $\tilde{k}$ in Eq. 2e or Eq. 4b is equal to 1.

From Eq. 6i, the maximum effective frequency ω_m must satisfy $\omega_m \geq (56.7\pi C_o/L) = 3.06$ rad/s (0.487 Hz). Suppose that $\omega_m = 5.4$ rad/s (=0.859 Hz). Then from Eqs. 6b and 6a, the sampling interval τ and the minimum resolution Δx for identification of the leak site and number M of the unit pipes become:

$$\tau = \frac{\pi}{\omega_m} = 0.924 \text{ s}, \quad \Delta x = \frac{\pi C_o}{2\omega_m} = 100 \text{ m}, \quad M = 200$$

Further, from Eq. 6l, we can choose N as follows: $(\omega_m L/\pi C_o) = 100 \ll N = 2{,}048$. From Eq. 6k, $\Delta\omega = 3.32 \times 10^{-3}$ rad/s ($=5.28 \times 10^{-4}$ Hz).

These parameters mean that the minimum resolution within which a leak can be identified becomes longer (100 m), and the frequency range for measurements becomes lower as the test zone of the pipeline becomes longer. Because acoustic waves of low frequency do not attenuate, even with the reduced resolution the method can be applied to a long pipeline.

If flow with a nonnegligible velocity (in comparison with the sound velocity) occurs, we would just multiply the frequency response in Eq. 2a by the term $\exp(-i\omega L/v')$ to yield the same outcome as if no flow occurred. The same procedure can be applied to the compensated frequency response to locate a leak.

Notation

A = cross-sectional area of the pipeline
$b(x, t)$ = fluid element velocity propagating backward
C_o = velocity of sound
C_b = total velocity of sound propagating backward
C_f = total velocity of sound propagating forward
C' = sound velocity when flow occurs in the pipeline
DFT = discrete Fourier transform
d = cross-sectional area of the leak
d_ℓ = diameter of a circular leak
$F(\ )$ = transfer matrix that characterizes the acoustic propagation in a pipeline
$f(x, t)$ = fluid element velocity propagating forward
f_{ij} = (i, j) element of the effective transfer matrix
$G(m)$ = transfer function estimated
$G(i\omega)$ = transfer function, the Fourier transform of $g(t)$
$g(k)$ = impulse response estimated

$g(t)$ = impulse response function
$g_i(t)$ = ith term of the function $g(t)$
IDFT = inverse discrete Fourier transform
i = imaginary unit
K = constant determined by the cross-sectional area of a leak
k = discrete time
$\tilde{k}$ = compensating coefficient of radiation impedance
L = length of the test zone of the pipeline
ℓ = site of the leak measured from the input side
ℓ^- = input site of ℓ
ℓ^+ = output side of ℓ
M = number of unit pipes
m = discrete frequency
N = number of data sampled
$P(x, i\omega)$ = Fourier transform of the sound pressure
$p(x, t)$ = sound pressure
$p_i(t)$ = sound pressure at the input site of the test zone
$p_o(t)$ = sound pressure at the output site of the test zone
Re = real part of complex numbers
t = time
t_ℓ = time when the pulse due to a leak occurs
t_L = time when the pulse occurs due to the constriction at the end of the test zone
$U(x, i\omega)$ = Fourier transform of the fluid element velocity
$u(x, t)$ = fluid element velocity
v = velocity of gas flow
v' = velocity of gas flow influenced by the sound velocity in the pipeline
$W(\cdot)$ = window function
x = distance from the input site of the test zone
Z_ℓ = radiational acoustic impedance of the leak
z = arbitrary variable

Greek letters

∂ = partial differentiation
ρ = density of gas
τ = sampling interval
ω = angular frequency
ω_l = lowest angular frequency of the signal considered
ω_h = highest angular frequency of the signal considered
ω_m = effective maximum angular frequency
$\Delta\omega$ = step size of angular frequency for discrete spectrum function

Symbols

$|\ |$ = absolute value

Literature Cited

Cole, E. S., "Methods of Leak Detection: An Overview," *J. Am. Water Works Assn.*, 73 (Feb., 1979).

Dallavalle, F., G. Possa, and F. Tonlini, "Early Leak Detection in Power Plant Feedwater Preheaters by Means of Acoustic Surveillance," *Symp. On-line Surveillance, Monitoring of Process Plant*, City Univ. London, p. 24.1 (Sept., 1977).

Decker, H. W., "Pipeline Leak Detection Using Nitrous Oxide Method," *ASNT Conf. (U.S.A.)*, 358 (1978).

Goldberg, D. E., "Transient Leak Detection," *7th Int. Pipeline Technol. Conf. (U.S.A.)*, 117 (1979).

Heim, P. M., "Leakage Detection on Buried Pipelines," *7th Int. Pipeline Technol. Conf. (U.S.A.)*, 169 (1979).

Huebler, J. E., N. C. Saha, and J. M. Craig, *Identification of Leaks—Internal Acoustic Techniques*, Report GRI-8010142, Inst. Gas Technol., Chicago (Aug., 1982).

Huber, D. W., "Real-Time Transient Model for Batch Tracking, Line Balance, and Leak Detection," *J. Con. Pet. Technol*, **20**(3), 46 (1981).

Lindsey, T. P., and J. C. Vanelli, "Real-Time Flow Modeling," *28th Ann. Pet. Chem. Ind. Conf. (U.S.A.)*, 189 (1981).

Parker, J. G., and A. N. Jette, "Surface Displacements Accompanying the Propagation of Acoustic Waves an Underground Pipe," *J. Sound Vibr.*, **69** (1980).

Ohizumi, J., et al., *Speech Synthesis, Lattice Pub. Co.*, Tokyo (1968).

Riemsdijk, A. J., and H. Bosserlaar, "On-Stream Detection of Small Leaks in Crude Oil Pipeline," *Proc. 7th World Pet. Cong.*, (1960).

Schmidt, G. K., and G. Lappus, "Dynamical Observers for State Reconstruction and Leak Detection in Natural Gas Pipeline Systems," *Proc. Jt. Auto. Control Conf. (U.S.A.)*, **1982**(2), TP6.E1 (1980).

Seiders, E. J., "Hydraulic Gradient Eyes In Leak Location," *Oil. Gas J. (U.S.A.)*, 77(47), 112 (1979).

Siebert, N., *Evaluation of Different Methods for Pipeline Leaking Monitoring*, Document of KFK-PDV-206, Kernforschungsanlage Juelich G.m.b.H. West Germany (Sept., 1981).

Siebert, H., and R. Isermann, "A Method for The Detection and Localization of Small Leaks in Gas Pipelines," *Automation for Safety in Shipping and Offshore Petroleum Operations*, 355 (1980).

Watanabe, K., "On Locating a Leak of Gas Transport Pipeline by Acoustic Method," *J. Fluid Control*, **14**(1), 39 (Mar., 1982).

Watanabe, K., and S. Sogo, "A Detection Method for Leak Location in a Gas Transport Pipeline by Use of Its Acoustic Characteristics," *Trans. SICE* (Japan), **16**(6), 885 (Dec., 1980).

Manuscript received May 6, 1985, and revision received Jan. 13, 1986.